available at www.sciencedirect.com

ScienceDirect

journal homepage: www.elsevier.com/locate/ijggc

Analysis and performance of oil well cement with 30 years of CO_2 exposure from the SACROC Unit, West Texas, USA

J.William Carey [a,*], *Marcus Wigand* [a], *Steve J. Chipera* [a], *Giday WoldeGabriel* [a], *Rajesh Pawar* [a], *Peter C. Lichtner* [a], *Scott C. Wehner* [b,1], *Michael A. Raines* [b,2], *George D. Guthrie Jr.* [a]

[a] *Earth and Environmental Sciences, Los Alamos National Laboratory, Los Alamos, NM, USA*
[b] *Kinder Morgan CO_2 Company, L.P., Midland, TX, USA*

ARTICLE INFO

Article history:
Received 31 July 2006
Accepted 17 August 2006
Published on line 28 December 2006

Keywords:
Sequestration
CO_2 enhanced oil recovery
Carbonation
Wellbore
Carbon storage

ABSTRACT

A core sample including casing, cement, and shale caprock was obtained from a 30-year old CO_2-flooding operation at the SACROC Unit, located in West Texas. The core was investigated as part of a program to evaluate the integrity of Portland-cement based wellbore systems in CO_2-sequestration environments. The recovered cement had air permeabilities in the tenth of a milliDarcy range and thus retained its capacity to prevent significant flow of CO_2. There was evidence, however, for CO_2 migration along both the casing–cement and cement–shale interfaces. A 0.1–0.3 cm thick carbonate precipitate occurs adjacent to the casing. The CO_2 producing this deposit may have traveled up the casing wall or may have infiltrated through the casing threads or points of corrosion. The cement in contact with the shale (0.1–1 cm thick) was heavily carbonated to an assemblage of calcite, aragonite, vaterite, and amorphous alumino-silica residue and was transformed to a distinctive orange color. The CO_2 causing this reaction originated by migration along the cement–shale interface where the presence of shale fragments (filter cake) may have provided a fluid pathway. The integrity of the casing–cement and cement–shale interfaces appears to be the most important issue in the performance of wellbore systems in a CO_2 sequestration reservoir.

1. Introduction

Developing confidence in methods of sequestering CO_2 in geological formations requires an improved understanding of the long-term sealing capacity of both the new and historical wellbore systems designed to prevent fluids from escaping the sequestration reservoir. The primary concern is that the Portland cements used to seal wellbores react readily with CO_2. This has led to the recognition that the long-term integrity of the wellbore seal is a primary performance issue in the geological sequestration of CO_2.

The potential effects of CO_2 on cement are varied and depend strongly on the extent of carbonation (Taylor, 1990). Moderate degrees of carbonation can be beneficial to cement porosity, permeability, and strength; extensive carbonation can result in the loss of cement structural integrity. The precise effects in the wellbore environment are difficult to predict because of uncertainties about the nature and extent

* *Corresponding author*. Tel.: +1 505 667 5540; fax: +1 505 665 3285.
E-mail address: bcarey@lanl.gov (J.W. Carey).
[1] Current address: Whiting Petroleum Corporation, Midland, TX, USA.
[2] Current address: PetroSource Energy Company, Midland, TX, USA.
1750-5836/$ – see front matter
doi:10.1016/S1750-5836(06)00004-1

of CO_2-saturated fluid interaction with the cement. Moreover, there is significant experimental variability in the interpretation of cement durability in the wellbore environment. Experiments of Duguid et al. (2005) and Barlet-Gouédard et al. (2006) suggest rapid carbonation, while those of Kutchko et al. (2006b) and our own unpublished experimental studies suggest more limited rates of CO_2 penetration and reaction.

CO_2-flooding operations in enhanced oil recovery provide a superb opportunity to investigate the medium-term (decades in length) performance of natural and engineered barriers to CO_2 migration. In this study, we investigated the impact of CO_2–cement interactions on cement performance by collecting wellbore samples from the world's second oldest continuous CO_2-flooding operation, the SACROC Unit, located in the Permian Basin of West Texas (Vest, 1970; Raines et al., 2001). CO_2 flooding operations at SACROC began in 1972. Since that time, 68 million metric tonnes of CO_2 have been effectively sequestered during an operation that recovers 38% of injected CO_2 for re-injection. Thirty million tonnes of the sequestered CO_2 is anthropogenic, derived by separation from the Val Verde natural gas field, making SACROC the largest demonstration of CO_2 sequestration in the world.

The SACROC Unit reservoir is located in a Pennsylvanian-age limestone reef (the Cisco and Canyon formations) with the Wolfcamp shale forming the caprock. The reservoir is located at about 2100 m depth; averages 240 m in thickness; and has a temperature and pressure of 54 °C and 18 MPa. Producing zones within the limestone reservoir have permeabilities in the 10–100 mD range and porosities near 10%, although these alternate with non-producing zones with permeabilities in the <0.1 mD range and porosities $<2\%$ (Raines and Helms, 2005).

The study location was well 49-6, located in the northern region of the reservoir. The well was drilled in 1950 to a total depth of 2131 m with the shale–limestone reservoir contact at 2000 m. Drilling mud additives varied with depth and included Aquagel (Na-montmorillonite), but from 1967–2000 m included only Tannex (tannin) and caustic soda (NaOH). Two sections of casing were run to total depth and separately cemented with a cement described only as Portland. It is probably a typical type 1, equivalent to API type A cement. The first stage circulated to surface from a depth of 534 m and included 6% addition of gel (presumably bentonite) with a density of 1678 kg/m^3. The second stage of cementing was to total depth and appears to be neat Portland cement (no additives given) with a density of 1857 kg/m^3. Following cementing, the producing zone was perforated at 15 intervals (the top-most was located from 2004 to 2009 m) and was acid stimulated with 477,000 L of HCl. The well was first exposed to CO_2 in 1975 and in subsequent years was a producer (relatively low pressure environment) for 10 years and an injector (relatively high pressure environment) for 7 years (a total of 110,000 tonnes CO_2 passed through the well).

2. Methodology

As part of Kinder Morgan's redevelopment of SACROC, a sidetrack core was obtained from well 49-6. The 5-cm diameter core was collected by re-entering the well and using a whipstock to guide the diamond core barrel out of the well, through the casing and cement and into the caprock. The sampled material extended from a depth of 1994 m to the shale–limestone reservoir contact at 2000.1 m. In addition, a cement bond log was collected for the depth interval between 1622 and 2075 m.

The core sample mineralogy and chemistry were characterized by quantitative X-ray diffraction (Chipera and Bish, 2002), X-ray fluorescence, and scanning electron microscopy. X-ray tomographic data were collected with a 125 kV, 66 μm beam with a 127 μm voxel resolution. Carbon and oxygen stable isotope data were obtained by phosphoric acid dissolution of solids with results reported in standard δ notation in parts per thousand relative to PDB. Air permeameter data were collected at atmospheric pressure on untreated and oven-dried samples (120 °C) as well as under confining pressure on oven-dried samples (65 °C) from 6.9 to 27.6 MPa. Porosity data were collected on solvent-cleaned (80% toluene and 20% methanol) and oven-dried (65 °C) samples. Computer modeling of cement degradation was conducted with the reactive transport code FLOTRAN (Lichtner, 2001) using the methods described by Carey and Lichtner (in press).

3. Results

The coring operation recovered samples of casing and cement from 6 to 4 m above the caprock–reservoir contact with the largest pieces about 10 cm in length. Shale was collected from 4 m above the contact down to the contact with the reservoir. Unfortunately, coring stopped just short of the limestone. As a proxy, we obtained a sample of limestone at the shale–reservoir contact from well 49-5, located about 0.6 km from well 49-6. A reconstructed cross-section of the wellbore environment is shown in Fig. 1 that includes the casing, cement, and shale caprock. The casing was in excellent condition and showed little evidence of corrosion. The cement was recovered in large pieces, although intact interfaces with the casing and caprock were not preserved as a result of coring operations. An additional 4 m of shale with abundant bedding-plane partings were recovered.

The recovered gray cement (>5 cm thickness) contains typical cement phases such as portlandite, ettringite, and katoite (hydrogarnet), a minor amount of calcite, and a substantial amount of amorphous material (Table 1). Halite is present in all samples and may be a residue of the brine. Two distinct alteration zones of the cement were observed: a dark rind (0.1–0.3 cm thickness) occurs between the casing and the cement and an orange-colored alteration zone of the cement (0.1–1 cm) occurs adjacent to the shale. The dark rind is a mixture of calcite, aragonite, and halite without a significant amorphous component. The orange zone is heavily carbonated cement and contains three polymorphs of $CaCO_3$(calcite, aragonite, and vaterite), halite, and a substantial amorphous component. Between the shale and the cement is a texturally complex region we have informally named the shale-fragment-zone (SFZ). This consists of a mixture of shale fragments, carbonated cement, and pure carbonates. Some analyses (not shown in Table 1) contain substantial dolomite.

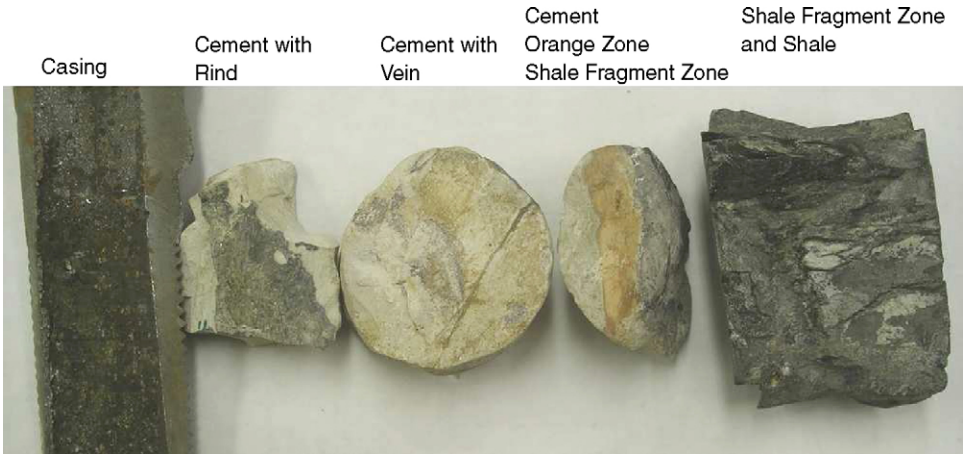

Fig. 1 – Photograph of samples recovered from well 49-6 showing the casing (left), gray cement with a dark rind adjacent to the casing, 5-cm core of gray cement, gray cement with an orange alteration zone in contact with a zone of fragmented shale, and the shale country rock.

Bulk chemical analyses by X-ray fluorescence demonstrate that the cement and orange zones have compositions differing primarily in the volatile ($H_2O + CO_2$) content and both materials have CaO–SiO_2–Al_2O_3–Fe_2O_3 values typical of Portland cement (Table 2). The shale composition is distinctly different from the relatively Ca-rich, Si-poor cement.

Detailed textural studies reveal a distinct asymmetry of CO_2 reactions. Against the casing, a relatively pure carbonate is deposited like a vein filling (Fig. 1). The gray cement adjacent to this deposit is only partially carbonated, retaining cement phases. In addition, the gray cement contains a set of subparallel calcium carbonate-filled fractures (Fig. 2). The cement adjacent to the shale caprock is intensely carbonated and altered to a distinct orange color. In SEM observations, the orange zone consists of a patchwork of calcium carbonate and Na–Al–Si cement residue. The interface between the cement and orange zone is characterized by a narrow (<1 mm), dark-gray deposit of layered amorphous silica, silica-carbonate, and carbonates (Fig. 7). This interface is denser than the gray cement or orange zone as shown in X-ray tomographic images (Fig. 3). On the caprock side of the cement, the interface between the orange zone and the caprock consists of a disturbed zone (the ''shale-fragment-zone'' or SFZ) which contains regions of high porosity (Figs. 4 and 5) and extraordinary reaction textures including agate-like layered deposits of silica and carbonate (Fig. 6).

Table 1 – X-ray diffraction data (in wt.%) for cement and shale samples from well 49-6 and limestone from well 49-5

Phase	Sample ID					
	1994.3[a](dark rind on cement)	1996.1[a] (gray cement)	1996.1[a] (orange zone)	1994.0-5.5[a] (SFZ)	1996.9[a] (shale)	1981.5[a] (limestone)
Portlandite	–	5.4	–	–	–	–
Katoite	–	5.1	–	–	–	–
Friedel's salt	–	0.6	–	–	–	–
Brownmillerite	–	1.5	–	–	–	–
Calcite	24	1.0	24	29	2.5	82
Aragonite	60	–	24	25	–	–
Vaterite	–	–	6.9	–	–	–
Dolomite	–	–	–	–	2.0	–
Ankerite	–	–	–	–	–	12
Quartz	–	–	–	0.1	22	3
Halite	14	0.3	0.9	1.4	0.1	0.5
Illite/smectite	–	–	–	31	62	3
Feldspar	–	–	–	–	5.1	–
Pyrite	–	–	–	–	3.4	0.2
Dawsonite	–	–	Trace(?)	–	–	–
Amorphous	Minor	86	44	14	2.3	–

Samples with qualitative amorphous values are normalized to 100%; ''illite/smectite'' includes phases identified as chlorite, kaolinite, and mica. Dawsonite tentatively identified by a single peak.
[a] Depth.

Table 2 – X-ray fluorescence analyses of samples from well 49-6 with depth in feet

Oxide	Depth			
	6545 (gray cement)	6549 (gray cement)	6549 (orange cement)	6551.5 (shale)
SiO_2	22.40	22.64	26.09	55.45
TiO_2	0.24	0.24	0.26	0.63
Al_2O_3	4.63	4.74	5.20	14.22
Fe_2O_3	2.52	2.56	2.74	5.70
MnO	0.11	0.11	0.10	0.03
MgO	3.46	3.68	1.36	2.63
CaO	62.94	62.23	58.90	4.03
Na_2O	2.24	1.93	4.29	0.95
K_2O	n.d.	n.d.	0.19	3.31
P_2O_5	0.10	0.10	0.10	0.10
LOI	18.67	19.16	35.26	11.24
Total	98.59	98.19	99.23	98.28

The analyses are in weight percent and have been normalized to a LOI-free basis (loss-on-ignition is the mass loss after firing at 1000 °C for 1 h; n.d. = below detection level).Typical type 1 Portland cement: SiO_2 (20.9%), Al_2O_3 (5.2%), Fe_2O_3 (2.3%), MgO (2.8%), and CaO (64.4%) Kosmatka and Panarese (1988).

The caprock is a dark, very fine-grained shale with thin quartz-rich layers separating clay-rich layers. The shale is fossiliferous and the clay layers are rich in dark-brown organic material. In thin-sections cut parallel to the layers, fossils and mud clast textures are evident. X-ray diffraction results (Table 1) show that the shale is predominantly illite and quartz with lesser amounts of feldspar, carbonate, pyrite, and other clay minerals. There is no obvious evidence for CO_2 interaction; the carbonate in the shale appears to derive from fossils and other primary, diagenetic features.

The limestone reservoir as sampled at well 49-5 is characterized by irregular lenses of shaley material in a calcite-rich matrix. The limestone is mostly calcite with lesser ankerite [$CaFe(CO_3)_2$] and quartz. The clay lenses are quite thin, being difficult to discern in thin-section, and are chlorite-rich with significant illite. We have not studied the reservoir rock in detail, but petrographically it consists of several generations of calcite, is rich in fossil textures and is very coarse-grained. Our cursory examination did not show obvious features associated with CO_2 injection (i.e., extensive dissolution of carbonates or precipitation of carbonates and/or dawsonite). The shale–limestone reservoir contact is abrupt and appears intact without obvious evidence of CO_2-induced reactions.

Carbon and oxygen stable isotope measurements of solid carbonates show distinct differences among elements of the wellbore cross-section (Fig. 8). Carbonates from the shale show typical marine $\delta^{13}C$ values. SFZ carbonates are slightly lighter in both carbon and oxygen. The carbonates in the orange-altered cement and the gray cement are distinctly different, while the carbonate vein deposit adjacent to the casing is similar to the orange-zone carbonates.

The porosity of the gray cement at 33.5% is typical for Portland cements, while the shale and the limestone (at well 49-5) have very low porosities (Table 3). The permeability of air-dried gray cement and orange zone samples were similar at 0.1 and 0.2 mD, respectively. Drying the samples at 120 °C caused extensive cracking of the gray cement and 200× higher permeability values. Interestingly, the orange zone did not fracture and had a relatively unmodified permeability. However, air-permeameter measurements conducted under confining pressures ranging from 6.9 to 27.6 MPa showed significantly reduced Klinkenberg-corrected permeabilities of 0.01 mD. The permeability of the shale was negligible perpendicular to the layers and near 9 mD parallel to the layers in oven-dried samples. The limestone sample had very low permeabilities (0.003 mD, Klinkenberg corrected) and porosity (2%).

The core bond log (CBL) shows that the occurrence of cement in the sampled interval was typical of well 49-6. Cement that is well bonded to both casing and the shale occurs from the contact with the limestone (2000 m) to 1950 m. Between 1950 and 1905 m, the cement distribution and bonding is more variable and includes a 5 m interval with little bonding or presence of cement. From 1905 to 1760 m, the cement is uniformly bonded to casing and formation. The CBL shows no evidence of CO_2-induced de-bonding or channel formation at or near the reservoir contact. Cement sections with potentially poor integrity are far removed from the reservoir and are likely to be features of the original cement job. The thick intervals of uniform cementing are consistent with a wellbore system that effectively isolates fluids of the reservoir.

4. Discussion

The most basic observation of the SACROC core is that at well 49-6 Portland cement survived and retained its structural integrity after 30 years in a CO_2-reservoir environment. While the cement permeability determined by air permeametry is greater than typical pristine Portland cement, it would still provide protection against significant movement of CO_2 through the cement matrix. The location of the sample at only 3–4 m above the reservoir contact suggests that the majority of the cement forming the wellbore seal has survived and would provide a barrier to fluid migration. The cement bond log supports this interpretation of the persistence of cement throughout the near CO_2-reservoir environment.

Fig. 2 – Polished slab showing gray cement with calcite-filled veins separated from the orange zone by a dark-gray interface. The shale-fragment-zone is visible at the right side. The casing is to the left-side (5 cm long).

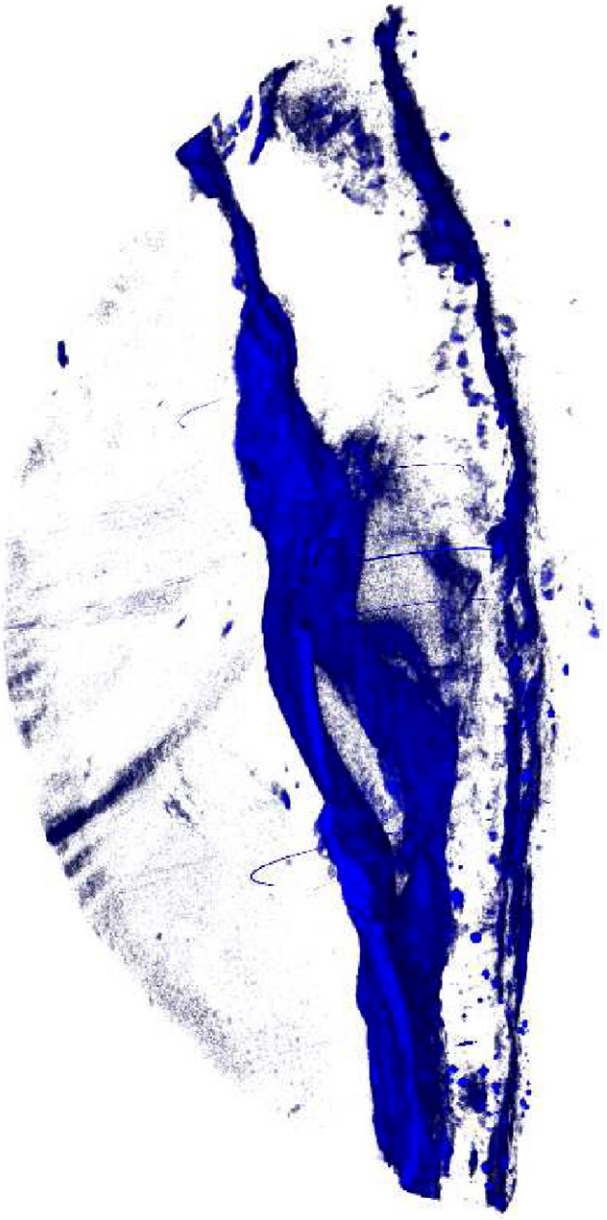

Fig. 3 – False-color X-ray tomographic image of the slab shown in Fig. 2. The image has been manipulated to render transparent all but the densest regions of the sample.

The coring operation produced cement fragments, the largest of which was 10 cm. This could indicate that the cement contained fractures downhole but was more likely due to the inherent stresses of the coring operation. In general, the broken surfaces of the cement core were not lined by alteration selvages demonstrating that these surfaces were not fluid pathways. The coring operation also recovered the casing, which showed minimal signs of corrosion. Given the 55-year age of the well, this is additional evidence that the cement retained its capacity to limit fluid circulation as steel corrosion is rapid in the absence of cement protection.

However, the cement core does contain features indicating extensive interaction with CO_2. At the casing–cement interface, calcite–aragonite occurs as a vein-filling deposit 0.1–0.3 cm in thickness (Fig. 1). We have not been able to determine whether the vein filled an existing space or if this deposit created its own space by the force of crystallization. The CO_2 leading to this deposit could have traveled along the casing–cement interface or it may have penetrated from inside the wellbore via the casing-threads or a point of corrosion. It is difficult to evaluate whether the casing–cement interface with carbonate vein was transmissive to CO_2 as we did not recover an intact casing–cement section. All appearances indicate that the dark rind fills the space between the cement and casing and would probably limit fluid flow.

The gray cement contains a sub-parallel set of healed-fractures that are filled with calcium carbonate (Figs. 1 and 2). The fractures may have developed in response to stresses caused by carbonation reactions at the casing and shale

Fig. 4 – Optical image of a porous opening in the SFZ showing a boxwork texture. Width of image about 1 mm.

Fig. 6 – SEM image of the SFZ. The diagonal hatchure defines the orange zone. Energy dispersive analyses are as follows: (A) Si; (B) Ca + Si; (C) Si; (D) Na + Al + Si; (E) Ca + Si.

interfaces, but their occurrence is not surprising given the likely stresses and potential differential pressures during injection and production. The calcium carbonate filling the fracture appears to limit potential transmissivity.

The gray cement contains calcite and aragonite in addition to portlandite [$Ca(OH)_2$]. The presence of portlandite is significant because it is well known to react rapidly to calcium carbonate. For example, experiments in our laboratories show that reagent portlandite, as-received, is partially carbonated (2.6%) and that carbonation proceeds to a significant extent (14%) if this material is exposed to humid air over the course of just 3 days at room temperature and atmospheric CO_2. The surviving portlandite in the gray cement of the SACROC core demonstrates that the gray cement cannot have experienced a pervasive flux of CO_2. The CO_2 that produced the small amount of carbonation in the gray cement probably arose by diffusion from either or both the casing and shale interfaces.

The orange zone is cement that has been extensively carbonated. All of the portlandite has been consumed and no other traces of crystalline cement phases such as katoite, brownmillerite, or Friedel's salt remain (Table 1). It does contain a substantial amorphous component ($\approx$ 50%) that accounts for the Al and Si of the original cement. Three polymorphs of calcium carbonate (calcite, aragonite, and vaterite) precipitated during carbonation. Aragonite and vaterite are both metastable relative to calcite and indicate strong supersaturation of the carbonating fluids, typical of cement–CO_2 interactions. Vaterite is very rare in natural carbonate rocks, but it is often reported in experimental studies of cement carbonation (e.g., Venhuis and Reardon, 2003). There is an intriguing indication of dawsonite as a single unexplained X-ray diffraction peak. This mineral is an often-predicted reaction product of CO_2 sequestration but its identification is tentative because of the low abundance.

Despite the extensive mineralogical changes, the orange zone is close in bulk composition to the gray cement (Table 2). The distinctive chemistry of cement rules out any significant possibility that the orange zone actually represents some

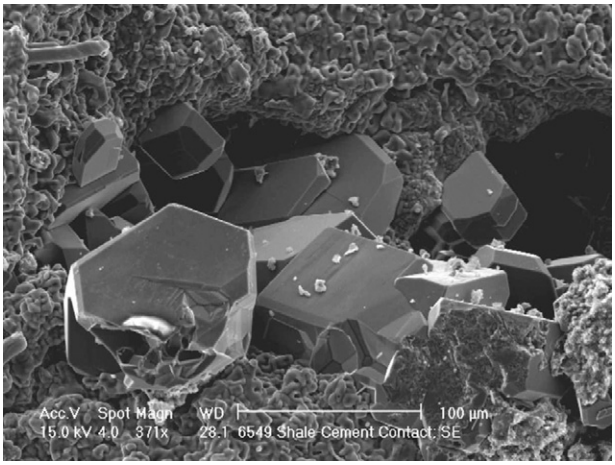

Fig. 5 – Crystals of calcite formed in void spaces like that shown in Fig. 4.

Table 3 – Porosity (in %) and air permeameter measurements (in mD) on shale, cement and orange zones from well 49-6

Sample	Permeability (mD)				
	Porosity	Air-dried	S.D.	Oven-dried	S.D.
Gray cement	–	0.09	0.02	17.6	18.8
Gray cement	33.5	–	–	0.016*	–
Orange zone	–	0.23	0.14	0.35	0.40
Shale ∥ layers	1.3			8.57	15.02
Shale ⊥ layers	–	–	–	<0.05	–
Limestone	2.2	–	–	0.003*	–

The limestone sample is from well 49-5. Oven-dried samples were measured after drying at 120 °C. Errors are based on data from seven locations on the cement and six locations on the orange zone. Permeameter data marked with * were made at 6.9, 59 and 27.6 MPa confining pressure and are Klinkenberg-corrected values.

other wellbore feature (e.g., filter cake). There are some notable minor variations in chemistry including a relative enrichment in SiO_2 and Na_2O and depletion in CaO and MgO. The alkali enrichment suggests that the carbonation process was associated with infiltration by brine. The alkaline-earth depletion and silica enrichment must reflect mass transport processes occurring with the CO_2 infiltration.

We have not made an extensive investigation of why the carbonated cement is orange in color. The iron content is similar in the gray cement and orange zone (Table 2); and, since the iron in the original Portland cement is completely oxidized, the orange zone is unlikely to reflect an oxidation of the gray zone. We and others have also observed a similar orange color in experimental brine–CO_2 reactions with cement (e.g., Duguid et al., 2005). We hypothesize that the carbonation process releases Fe^{3+} from complex hydrated Ca-bearing cement phases and reacts to form amorphous iron hydroxides (e.g., Taylor, 1990). This amorphous material may provide the orange color.

The orange zone is variable in thickness and ranges from 1 cm to a few mm. We have not been able to obtain conclusive evidence on whether this alteration zone is continuous within the wellbore environment. The orange zone samples extend for 30–40 cm of the recovered core. By considering the geometry of the whipstock coring operation, the extent of the recovered orange zone samples is about as expected for a continuous reaction zone. It is also apparent that the orange zone could not be significantly thicker elsewhere as a greater extent of altered cement would have been recovered.

The gray cement and orange zones are separated by a dark translucent interface (Figs. 2 and 7). The interface is variable in thickness and splits along its length to form other interfaces within the orange zone. These internal interfaces may reflect a succession of carbonation fronts moving into the gray cement. The interface is dense in appearance and X-ray tomographic studies demonstrate that the layer is denser than either the gray cement or orange zone and that it appears to form a continuous barrier (Fig. 3). We hypothesize that this interface could limit the rate of CO_2 migration into the gray cement (explaining the persistence of portlandite) and also limit the depth of penetration of the intense carbonation zone.

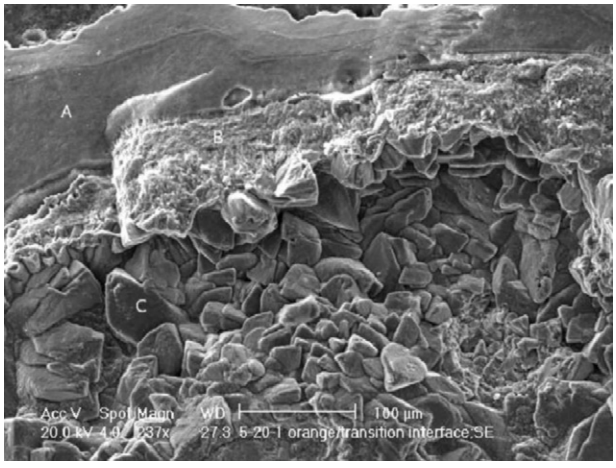

Fig. 7 – SEM image of the interface between the orange and gray cements. Upper smooth region (A) contains only Si. The intermediate, rough layer (B) is Si + Ca. The distinct crystals (C) are dolomite. The orange zone is towards the top of the image.

The shale-fragment-zone, which occurs at the interface between the orange zone and the shale caprock, is the most complex of the samples recovered from well 49-6. It is characterized by black fragments of shale (which have split along bedding planes) embedded in a gray, carbonate-rich, fine-grained matrix. Unfortunately, none of the recovered samples spans the orange zone to shale region and we can only estimate that the thickness of the SFZ does not appear to exceed about 0.5 cm. The mineralogy and textures suggest that the SFZ matrix is composed of drilling residue mixed with cement. Another important feature of the SFZ are some regions of open porosity (Figs. 4 and 5).

What is more puzzling is that the SFZ has extraordinary reaction textures indicative of extensive chemical mobility (Fig. 6). Layers and bands of pure silica and pure calcium (or dolomitic) carbonate occur together and separately. Large sinuous regions of silica occur as well as pockets or void spaces lined with silica and carbonate. The SFZ–orange zone contact is in many places distinct and planar but in one location there is a prominent wedge of SFZ that intrudes (or is intruded by) the orange zone (Fig. 6). The matrix of the SFZ consists of very fine-grained calcite, aragonite, dolomite, silica, and a significant amount of halite.

The evidence for silica mobility in the SFZ was unexpected. The solubility of silica is limited in the low pH environment generated by carbonic acid as well as in the Ca-rich, high-pH cement environment. The silica may have been mobilized and moved out of the cement zone as a part of the carbonation process (see Section 5). One other possibility is that the use of NaOH in the drilling mud could have generated a corrosive environment capable of dissolving silicate and generating some of the deposits observed in the SFZ.

The geometry, mineral distribution, and textural character of the orange-zone carbonation suggest that the origin of the CO_2 was via migration from the reservoir along the cement–shale interface. As shown in Fig. 2, the interface between the gray and orange cements is approximately parallel to the wellbore and parallel to the shale–cement contact. This geometry essentially eliminates the possibility that the CO_2 has infiltrated through the cement matrix from the reservoir as this would require partitioning of the fluid along the outer boundary layer of the gray cement.

Rather, the geometry suggests that the CO_2 infiltrated the cement from the contact with the shale, perpendicular to the interface. The source of the CO_2 at the cement-shale interface is not likely to be via migration along the shale bedding planes but rather from the limestone reservoir via the shale-fragment-zone. This interface consists of shale fragments that may have prevented the cement from forming a tight seal with the shale wall. Optical microscopy and SEM show that the SFZ still retains porosity with open veining that may have facilitated movement of CO_2 (Figs. 4 and 5). The CO_2 could have occurred dissolved in the brine or as a separate supercritical phase or a combination of the two. Our bulk composition data demonstrate that the carbonation process did involve movement of Si, Na, Ca, and Mg. Since a pure

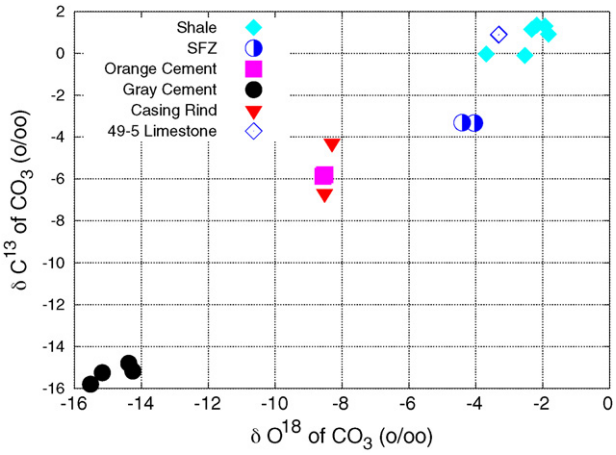

Fig. 8 – Carbon and oxygen isotope measurements of solid carbonates in samples illustrated in Fig. 1.

supercritical CO_2 phase is unlikely to move these elements, an aqueous diffusion process appears to be involved.

With a model of CO_2 carbonation proceeding from the SFZ, the interface between the gray and orange cement represents the carbonation front as it progresses inwards from the contact with the shale. As discussed previously, the dense, silica-rich character of the interface may have helped to slow the advance of the front and may have helped to prevent significant carbonation of the interior gray cement.

The CO_2 that migrated along the SFZ was most likely derived from the injected and produced CO_2 associated with enhanced oil recovery (EOR) activities. A second possible, limited-term, limited-volume source is the acid stimulation of the limestone reservoir conducted during well completion (see Section 1). The amount of CO_2 generated by acid stimulation is likely to have been relatively small (477,000 L of 15% HCl could produce a maximum of 47 metric tonnes of CO_2), but it would have occurred early in the life of the wellbore, perhaps prior to complete curing of the cement. At this point, we cannot demonstrate that all of the CO_2 producing the orange zone was derived from CO_2-EOR.

The isotopic data show distinct differences in the carbon values for weakly carbonated gray cement compared to the orange altered cement and casing-interface deposit (Fig. 8). There is some cement literature on the isotopic behavior of cement carbonation that suggests, unfortunately, that kinetic factors are very important in determining isotopic fractionation (Rafai et al., 1991). The kinetic studies show that carbon and oxygen isotopes continuously evolve over a period of months. In view of these complexities, a more thorough analysis will be presented in the future following a more complete study of fluid and gas isotope chemistry. The existing data are consistent with the interpretation of the gray cement experiencing a different type of CO_2 exposure from either the orange zone or the casing-interface. We suggest that this difference may reflect the extent of CO_2 exposure: the gray cement was in a CO_2-poor environment and perhaps relatively unequilibrated with the infiltrating CO_2, while the orange alteration zone and the casing–cement interface were in a CO_2-rich environment and relatively more equilibrated.

5. Numerical modeling

In order to improve our understanding of the carbonation process and as a step in the development of a predictive model for cement degradation, we conducted numerical simulations of CO_2–cement interactions using the reactive transport code FLOTRAN (Lichtner, 2001). Our conceptual model, following the previous discussion, is that CO_2-saturated brine percolated up the cement–shale interface and in so-doing equilibrated with the shale mineralogy while maintaining a high effective CO_2 pressure. As the fluid migrates upward, CO_2-saturated brine diffuses into the cement matrix. This two-dimensional problem was simplified to a one-dimensional representation which consisted of a column of shale and CO_2-saturated brine in contact with a fully cured, CO_2-free cement paste (for more details see Carey and Lichtner, in press).

The initial conditions were a fully hydrated, CO_2-free cement (0.05 m in length with porosity = 30%) adjacent to a porous, carbonate-bearing shale-fragment zone (0.2 m in length with porosity = 70%). The choice of a large, high porosity shale volume was designed to simulate a steady source of CO_2-saturated brine from the reservoir through the high porosity SFZ. The brine in the SFZ was saturated with 18 MPa CO_2 and the calculations were conducted at 25 °C rather than 50 °C because of thermodynamic database limitations. The initial cement mineralogy was 38% calcium silicate hydrate (with Ca/Si = 1.78), 15.4% portlandite, 13.5% monosulfate, 3.3% hydrogarnet, and 30% porosity. The initial SFZ mineralogy was taken as 19.8% illite, 6.6% quartz, 1.3% albite, 1.0% kaolinite, 0.7% calcite, 0.7% dolomite, and 70% porosity. The calcium silicate hydrate phase was modeled as a kinetically controlled solid solution between $Ca(OH)_2$ and SiO_2 using the methods of Lichtner and Carey (2006).

In the simulations, the key variables controlling reaction characteristics were the tortuosity and porosity of the cement and reaction rates of the minerals. These were adjusted in an effort to reproduce the primary mineralogical and compositional features of the orange alteration zone after 30 years of CO_2 exposure.

The simulation captures several key features of the observed reactions at SACROC such as the width of the carbonation zone, carbonate deposition, cement alteration, interface formation, and compositional variation (Figs. 9–12). The simulation reproduces the loss of all primary cement phases in a 0.005 m region adjacent to the shale interface (Fig. 9) and their replacement by a mixture of calcium carbonate (Fig. 10; we did not attempt to model the kinetics of aragonite and vaterite), amorphous silica (Fig. 10), and amorphous aluminum hydroxides (Fig. 11; represented by gibbsite in the model). The constraints of the diffusion-based model showed that it was necessary to have the effective porosity of the SFZ greater than the shale to reproduce the penetration of the reaction front (if the porosity of the SFZ was less than the cement, the reaction front moved to the original interface and into the SFZ; see Carey and Lichtner (in press) for additional details).

The depth of the reaction front penetration was a sensitive function of the cement tortuosity. A value of 0.0004 (implying a very convoluted diffusion path) was necessary to limit the reaction front to the observed 0.005 m. The sharpness of the

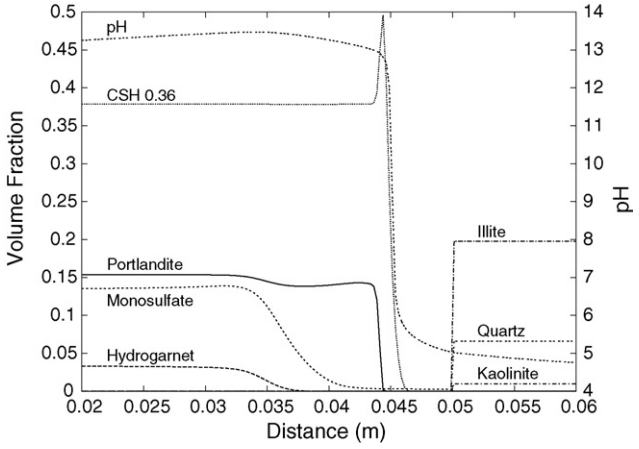

Fig. 9 – Calculated mineralogical and pH profile across the carbonation zone for the primary cement and country rock phases at 30 years. The initial cement–shale interface is at 0.05 m. None of the primary cement phases survive in the alteration zone between ≈ 0.046–0.05 m.

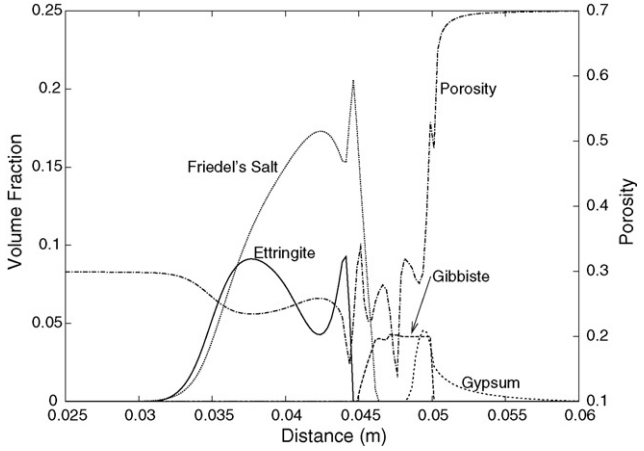

Fig. 11 – Calculated mineralogical and porosity profile across the carbonation zone for aluminous and sulfate-bearing minerals at 30 years. The initial cement–shale interface is at 0.05 m.

reaction front was sensitive to reaction rates with too slow a rate producing uniform alteration and too fast a rate producing a very narrow reaction front. We did not attempt to model surface areas explicitly (e.g., through the use of geometric surface areas and average particle sizes) and instead chose a product of the surface area and intrinsic rate constant that provided the most reasonable fit; these values varied between 1×10^{-10} mol/s for calcite to 1×10^{-12} mol/s for ettringite. In order to suppress significant precipitation, the kinetic rates for dawsonite, albite, illite, kaolinite, and quartz were 1×10^{-20} mol/s, as we do not expect significant reaction of silicates during the 30 years of CO_2 exposure.

The numerical simulation is also able to reproduce the dense interface between the gray cement and orange zone (Fig. 2). During carbonation, the calcium silicate hydrate phase

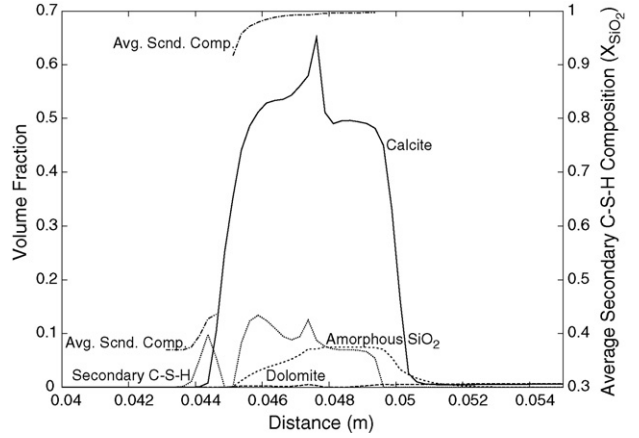

Fig. 10 – Calculated mineralogical profile across the carbonation zone for secondary carbonate and siliceous minerals at 30 years. The initial cement–shale interface is at 0.05 m. Note discontinuity in the average composition of the secondary C–S–H precipitate.

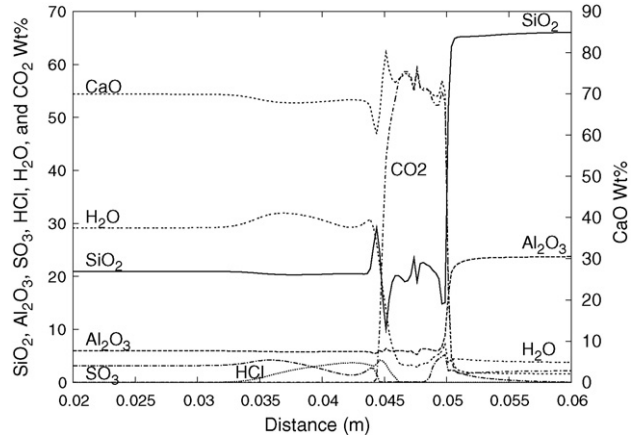

Fig. 12 – Calculated compositional profile across the carbonation zone at 30 years. The initial cement–shale interface is at 0.05 m. Compositional data and mineralogical controls for Na_2O, K_2O, and MgO were not modeled.

is enriched in abundance from 38 to 56% at the interface (sum of CSH 0.36 and ''Secondary C–S–H'' in Figs. 9 and 10) and is also partially decalcified (see composition axis in Fig. 10). This deposition is associated with a reduction in porosity from 30 to 18% (Fig. 11). Although less distinct in the simulation, the model also predicts the mobilization of amorphous silica into the SFZ (Fig. 10), which may account for some of the observed silica deposits (Fig. 6).

The compositional trends across the carbonation zone were sensitive to the porosity model. The results shown in Fig. 12 are relatively uniform in composition in agreement with observations (Table 2), whereas alternative porosity distributions resulted in parts of the reaction zone completely lacking Si or Al.

We did not observe the distinct peaks and valleys predicted in the abundances of phases such as calcite or Friedel's salt or in the porosity and bulk compositional data. We believe that

the detail predicted in the 1D model would probably be smoothed out in a 3D model which had an initial heterogeneous mineralogical and compositional distribution as is likely in real cement. Other shortcomings of the model include the prediction of gypsum (Fig. 11) which was not observed and the prediction that the cement interior is completely unaltered contrary to the observation of calcium carbonate in the gray cement. However, the gray cement may also have had CO_2 infiltration from the casing interface.

Finally, we should note that some of the derived model parameters, such as tortuosity and reaction rates, are dependent on the nature of the model. For example, a more complete 2D model could allow a more limited or episodic exposure of the cement to CO_2 via the SFZ. In these conditions, the tortuosity required to limit the depth of CO_2 penetration could have been substantially reduced.

6. Conclusions

The Portland cement recovered from a 55-year old well with 30 years of CO_2 exposure showed evidence of exposure to CO_2 in the form of carbonate precipitate adjacent to the casing and heavily carbonated, orange-colored cement adjacent to the shale caprock. However, the structural integrity of the recovered cement core, petrographic observations, air permeameter data, and cement bond log indicate that the cement retained its capacity to prevent significant transport of fluid through the cement matrix. Observations and numerical calculations suggest that the CO_2 producing the orange alteration originated by movement from the reservoir along the shale–cement interface. The CO_2 producing a carbonate precipitate at the casing–cement interface may have originated by migration along the casing interface from the reservoir or from the interior of the well at casing joints or regions of casing corrosion.

Numerical modeling shows that carbonation induced by diffusion of CO_2-saturated brine reproduces key features of the SACROC cement core. We used observations of the core to constrain the porosity, tortuosity, and reaction rates used in the modeling to values appropriate to well 49-6 at SACROC. Additional samples would be necessary to construct a more generally applicable model of CO_2-induced cement degradation.

The observations demonstrate that Portland cement can retain its integrity at least over decades in a CO_2 reservoir with conditions similar to SACROC. Numerical calculations are consistent with a slow rate of degradation by diffusive attack of CO_2 that would allow a thick column of cement to survive for long periods of time. However, the observations also show that CO_2 migrated along the casing–cement and shale–cement interfaces for some period of time. We were unable to quantify the amount of CO_2 migration that may have occurred along these interfaces. The integrity of these interfaces appears to be the most critical issue in wellbore performance for CO_2 sequestration.

The cement core recovered at SACROC provides some help in understanding the experimental variability in studies of cement carbonation at reservoir conditions. The laboratory experiments of Duguid et al. (2005) investigated cement deterioration under conditions of flowing CO_2-saturated brine and they observed rapid degradation and loss of structural integrity within weeks of exposure. The SACROC sample clearly did not experience a similar flux of acidic brine. This indicates that for properly completed wells, the cement–caprock interface does not experience flowing CO_2-saturated brine and the rapid cement decomposition observed by Duguid et al. (2005) is unlikely to occur.

In contrast, the experiments of Barlet-Gouédard et al. (2006) and Kutchko et al. (2006b) were conducted with a static volume of brine subject to high CO_2 pressure. Barlet-Gouédard et al.'s experiments were conducted at 90 °C and 28 MPa, and they observed rapid penetration of CO_2 and complete carbonation within 6 weeks. Their porosity and mechanical strength studies showed that the cement appears to retain significant hydrologic integrity but had clearly been substantially altered. Kutchko et al.'s experiments were conducted at 50 °C and 30 MPa and showed very limited (slow) penetration of CO_2 after 9 days (and after 3 months as presented in Kutchko et al., 2006a). The SACROC cement samples (exposed to CO_2 at 54 °C and 18 MPa) showed rates of carbonation more compatible with the experiments of Kutchko et al., which may reflect the more similar temperatures of CO_2 exposure. However, it also possible that the amount of CO_2 exposure for the SACROC samples at 3 m above the reservoir contact was more limited. The time and conditions for cement curing times prior to CO_2 exposure is another important variable: SACROC at 35 years (54 °C) compared to Kutchko et al. at 28 days (22 and 50 °C) and Barlet-Gouédard et al. at 2 days (90 °C). In any case, both the Barlet-Gouédard et al. and Kutchko et al. studies are consistent with cement retaining hydrologic integrity in a CO_2-rich environment, although the results of Barlet-Gouédard et al. indicate that CO_2-induced cement degradation in higher temperature reservoirs may be of greater concern.

The SACROC core in combination with the available experimental data allow some preliminary conclusions regarding wellbore integrity and CO_2 storage. These studies indicate that Portland cement based wellbore systems, if properly completed, can prevent significant migration of CO_2 from reservoirs for long periods of time (at least decades). A properly completed well need not be completely free of defects, but should not have continuous openings along either the cement–casing or cement–caprock interfaces that might permit a CO_2–brine mixture to flow that could dissolve cement and further widen the interface. The key variables appear to be the initial width and connectivity of the interfaces in addition to the pressure gradient driving flow from the reservoir.

Future work to develop and strengthen these conclusions should include collecting additional core to understand whether the observations at well 49-6 are unique or typical at SACROC and to explore the significance of differing caprock and reservoir chemistries as well as differing operational histories. These studies could improve on our work by obtaining fluid samples to better constrain the geochemistry and collecting samples at multiple intervals to determine the maximum extent of carbonation. In addition, more experimental studies are needed to help interpret the field observations. These should focus on the evolution of cement-casing and cement–caprock interfaces as a function of initial interface width/quality and the CO_2–brine flux. Observations at

SACROC suggest that under limited flux the interfaces may be self-sealing. Determining the conditions under which these interfaces become more transmissive with time remains a key unknown in evaluating the longevity of the Portland cement seal in wellbore systems.

Acknowledgements

We are grateful to Melissa Fittipaldo for electron microscopy, Toti Larson for stable isotope analyses, and Tim Ickes for X-ray tomography (all at Los Alamos National Laboratory); to Bob Svec for air permeameter measurements (at New Mexico Tech); and Chandra Rai for porosity and air permeameter measurements (at University of Oklahoma). Kinder Morgan CO_2 Company is gratefully acknowledged for providing the core samples used in this study. This work was supported by LDRD-DR 2004042DR and the U.S. Department of Energy–NETL Contract #04FE04.

REFERENCES

Barlet-Gouédard, V., Rimmelé, G., Goffé, B., Porcherie, O., 2006. Mitigation strategies for the risk of CO_2 migration through wellbores. In: Proceedings of the IADC/SPE Drilling Conference, February 21–23, Miami, Florida, SPE 98924-MS.

Carey, J.W., Lichtner, P.C., in press. Calcium silicate hydrate solid solution model applied to cement degradation using the continuum reactive transport model FLOTRAN. Am. Ceram. Soc., Mater. Sci. Concrete.

Chipera, S.J., Bish, D.L., 2002. FULLPAT: a full-pattern quantitative analysis program for X-ray powder diffraction using measured and calculated patterns. J. Appl. Crystallogr. 35, 744–749.

Duguid, A., Radonjic, M., Scherer, G., 2005. Degradation of well cements exposed to carbonated brine. In: Fourth Annual Conference on Carbon Capture & Sequestration, May 2005, Alexandria, VA.

Kosmatka, S.H., Panarese, W.C., 1988. Design and Control of Concrete Mixtures, 13th ed. Portland Cement Association.

Kutchko, B.G., Strazisar, B.R., Dzombak, D.A., Lowry, G.V., 2006a. Degradation of well cement under geologic sequestration conditions. In: 2nd Wellbore Integrity Network Meeting, Princeton, New Jersey, March 2006. http://www.co2captureandstorage.info/networks/wellbore.htm.

Kutchko, B.G., Strazisar, B.R., Dzombak, D.A., Lowry, G.V., Thaulow, N., 2006b. Degradation of wellbore cement by CO_2 under geologic sequestration conditions. Environ. Sci. Technol., submitted for publication.

Lichtner, P.C., 2001. FLOTRAN User Manual. Tech. Re LA-UR-01–2349, Los Alamos National Laboratory.

Lichtner, P.C., Carey, J.W., 2006. Incorporating solid solutions in geochemical reactive transport equations using a kinetic discrete-composition approach. Geochim. Cosmochim. Acta 70, 1356–1378.

Rafai, N., Létolle, R., Blanc, P., Person, A., Gégout, P., 1991. Isotope geochemistry (^{13}C, ^{18}O) of carbonation processes in concretes. Cement Concrete Res. 21, 368–377.

Raines, M.A., Dobitz, J.K., Wehner, S.C., 2001. A review of the Pennsylvanian SACROC Unit. In: Fall Symposium West Texas Geological Society, October 24–25.

Raines, M.A., Helms, W., 2005. Non-standard core analysis applied to geologic model generation for fluid flow simulation. In: Lufholm, P., Cox, D.M. (Eds.), Unconventional Reservoir, Technology, and Stratgies: Alternative Perspectives for the Permian Basin, No. 05–115. West Texas Geological Society, Midland, Texas, pp. 123–136, 2005 WTGS Fall Symposium.

Taylor, H.F.W., 1990. Cement Chemistry. Academic Press, London.

Venhuis, M.A., Reardon, E.J., 2003. Carbonation of cementitious wasteforms under supercritical and high pressure subcritical conditions. Environ. Technol. 24, 877–887.

Vest, Jr., E.L., 1970. Oil fields of Pennsylvanian–Permian Horseshoe Atoll, West Texas. In: Halbouty, M.T. (Ed.), Geology of Giant Petroleum Fields, vol. 14 of Memoir—American Association of Petroleum Geologists, 185–203.